Estimation of Finger Joint Angle from Single-channels sEMG Based on Improved Backpropagation Neural Network Model

Lei Zhang, Ruifeng Wang, Hui Zhao

***Abstract* — Currently, accurate estimation of finger movements typically relies on multi-channel surface electromyography (sEMG) signals. However, the multi-channel sEMG signals face many problems and challenges. This paper proposes a new method. It uses a single-channel sEMG signal and combines backpropagation neural networks (BPNN) with singular spectrum analysis (SSA) to accurately estimate the joint movement of four fingers. Experimental results show that the single-channel sEMG signals based on the BPNN_SSA method can effectively estimate the joint movement of four fingers, with an average R^2 of 0.758 and an average NRMSE of 18.9%. Compared to other methods, signals estimated using BPNN_SSA demonstrate higher stability and are closer to the measured signals of four-finger joints. Thus, this study indicates the feasibility of estimating four-finger joint movement based on single-channel sEMG .**

***Index Terms* — Estimation of finger movements, Single-channel surface Electromyography, Backpropagation neural networks, Singular spectrum analysis.**

I. Introduction

Human-robot interaction (HRI), as a cutting-edge research field, has achieved large-scale applications in manufacturing, aerospace, education, military, and healthcare scenarios [1-3].

In modern HRI technology, surface electromyography (sEMG) signals are commonly used as bioelectrical signals. Compared with other signal acquisition methods, sEMG has advantages such as high resolution, mature acquisition technology and non-invasive data acquisition [4]. Currently, sEMG is primarily used for transmitting motion commands in assistive devices, encompassing key applications such as prosthetic control, exoskeleton actuation, and rehabilitation robot control [5-10]. Especially in the field of rehabilitation medicine, sEMG, by representation of human motor intentions [11,12], has become a pivotal technological support for predicting dynamic prosthetic joint angles, generating exoskeleton gait patterns, and planning continuous motion for rehabilitation robots.

In the continuous estimation of sEMG signals, biomechanical models and machine learning regression models are two primary methods for establishing the relationship between these signals and human movement [13]. Biomechanical models tend to be complex and involve multiple biological parameters that cannot be directly measured, which presents practical challenges in their application [14]. Consequently, many researchers prefer machine learning approaches [15,16] to create a relationship between sEMG signals and movements. Qin *et al.* [17] introduced a continuous forecasting model for multiple joints of the forearm utilizing Convolutional Neural Networks (CNN), attaining correlation coefficients up to 0.9 as an evaluation benchmark. Zhang *et al.* [18] proposed a model for continuously predicting lower limb joint angles using long short-term memory neural networks. Nevertheless, existing continuous estimation prediction models inevitably exhibit errors and fluctuations during predictions, thereby impacting the accuracy of joint angle estimations. As a result, Some researchers have employed smoothing techniques to mitigate these issues. For instance, Qin *et al.* [19] applied singular spectrum analysis within their prediction model to smooth forecasted angles effectively. Similarly, Wang *et al.* [20] utilized artificial neural networks for smoothing purposes in their predictive model. Therefore, incorporating appropriate smoothing techniques is crucial for enhancing the accuracy of continuous estimation predictions.

Various methods for estimating human continuous joint motion using multi-channel sEMG have been developed recently. Wang *et al.* [21] introduced a general neural network model for regression, which employs a genetic algorithm to establish predictions of knee joint angles using multi-channel sEMG signals. Similarly, Xiao *et al.* [22] chose time domain features and proposed a grey feature weighted support vector machine to build a model that relates sEMG signals to elbow joint angles. Although multi-channel sEMG signals demonstrate considerable potential in joint motion estimation, their practical application remains constrained by critical issues such as muscle state instability, mechanical/signal interference, and increased system complexity. Consequently, current research is increasingly focused on utilizing sEMG signals from a limited number of muscles or a solitary muscle to enhance the effectiveness of human motion estimation while addressing challenges related to operational convenience and system complexity [23].

Compared with multi-channel sEMG signals, single-channel sEMG signals have the advantages of simpler equipment, lower cost, lower computational complexity and time requirements. Recently, there has been an increase in research focused on single-channel sEMG signals. Zhang *et al.* [24] proposed a method for estimating knee joint

Manuscript received September 10, 2024; revised February 16, 2025

This research was partially funded by the Natural Science Basic Research Project 2022JQ-397 of Shaanxi Province and the Science and Technology Project GX2307 of Xi 'an North Forest District.

Zhang Lei is an assistant professor at the School of Mechatronic Engineering, Xi'an Polytechnic University China. (Email:20201205@xpu.edu.cn)

Wang Ruifeng is a graduate student at the School of Mechatronic Engineering, Xi'an Polytechnic University China. (Email:1711461153@qq.com)

Zhao Hui is a graduate student at the School of Mechatronic Engineering, Xi'an Polytechnic University China. (Email:1760964837@qq.com)

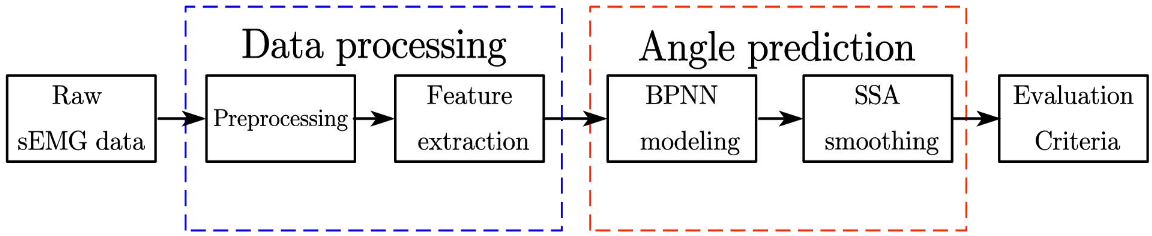

Figure 1. Flowchart of the processing procedure.

motion utilizing a state-space model based on single-channel sEMG signals. Zhang *et al.* [25] also introduced knee joint motion estimation through feature-guided CNN applied to single-channel sEMG signals. Shao *et al.* [26] employed wavelet deep belief networks with single-channel sEMG to recognize upper limb motions. Wu *et al.* [27] recognized gestures by analyzing envelope signals derived from single-channel sEMG. However, existing research on single-channel sEMG signals has primarily focused on the recognition of discrete movement patterns. In contrast, the exploration of their application in continuous motion estimation, particularly for multi-joint continuous movements of the fingers, remains a largely unexplored area. To bridge this, this paper proposes an approach that utilizes a Back Propagation Neural Network (BPNN) enhanced through Singular Spectrum Analysis (SSA), attempting for the first time to estimate the continuous joint angles of four fingers by employing single-channel sEMG. In order to assess the method's efficacy, the experimental design adopts a multi-position evaluation strategy, conducting a comparative analysis of four-finger movement predictions at multiple sEMG acquisition points on the forearm. Notably, traditional machine learning models commonly suffer from output fluctuation issues during continuous movement angle prediction. To mitigate this limitation, this study introduces SSA signal smoothing techniques, effectively suppressing prediction noise through a "decomposition-reconstruction" signal processing approach. Experimental results show that the single-channel sEMG estimation method based on BPNN_SSA can not only effectively predict four-finger movements but also outperforms traditional machine learning models applied directly in terms of prediction performance.

The contribution of this article is as follows:

1. The four-finger continuous motion prediction was achieved using single-channel sEMG signals.

2. The performance of the four-finger continuous motion prediction model was improved by adopting a smoothing processing method.

Figure 1 illustrates this article's signal processing workflow. The remaining sections are structured : Section 2 covers the experimental setup and methods, including signal collection, preprocessing, feature extraction, modeling for angle estimation from sEMG, and evaluation metrics. Section 3 presents the experiments and results, while Section 4 provides a discussion of the research. Section 5 draws the conclusions.

II. Materials and Methods

A. Experimental protocol

This study selected five healthy participants (three males and two females, aged 22-25) with no history of neurological or muscular disorders. All experimental procedures received approval from the medical and experimental animal ethics committee at Northwestern Polytechnical University. Participants were informed that the experiments posed no harm, and they provided signed informed consent forms. The locations of the sEMG signals during the experiment are illustrated in Figure 2(b). EMG sensors were placed on six muscles: Extensor Digitorum Communis (EDC), Flexor Digitorum Superficialis (FDS), Flexor Carpi Radialis (FCR), Flexor Carpi Ulnaris (FCU), Extensor Carpi Radialis (ECR), and Extensor Carpi Ulnaris (ECU). sEMG sensors with a sampling frequency of 1000 Hz were utilized, as depicted in Figure 2(c). The data acquisition card employed was the USB-4704 from Advantech. Additionally, an Inertial Measurement Unit (IMU) was used to measure angle data for the collective movement of four fingers at a sampling rate of 100 Hz, as shown in Figure 2(d). The experimental setup is presented in Figure 2(a). Before collecting surface EMG signals, participants maintained still postures with relaxed muscles to avoid muscle tension. Additionally, the wrist, elbow, and shoulder joints were kept stable to ensure that any potential movement in these positions did not interfere with the collected sEMG signals. As illustrated in Figure 2(e), during sEMG signal acquisition, fingers began from a naturally relaxed state while only engaging in simultaneous extension and flexion movements at the four finger joints. After two minutes of motion, the fingers returned to their naturally relaxed position. Each participant repeated this experimental process five times, with a two-minute break between consecutive trials to minimize the impact of muscle exhaustion.

B. SEMG signal processing

1) SEMG signal denoising

sEMG signals are feeble, typically exhibiting amplitudes ranging from 100 to 5000 μV, peak-to-peak values between 0 and 6 mV. The effective frequency spectrum of sEMG lies within the range of 20 to 500 Hz, with a significant concentration in the interval of 50-150 Hz. Consequently, it is essential to denoise the raw sEMG signals to obtain reliable data for analysis. This study employed a notch filter to eliminate the interference at 50 Hz, followed by bandpass filtering within the range of 20-450 Hz.

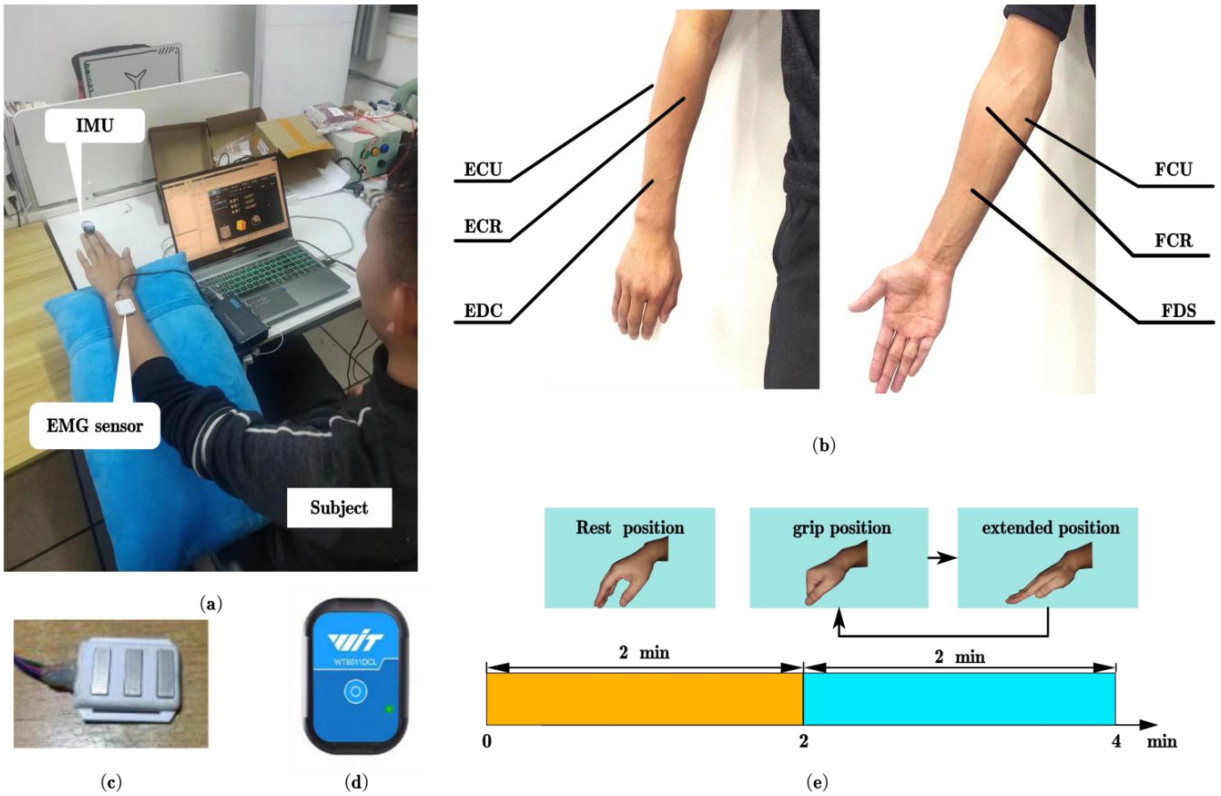

Figure 2. Experimental Setup: (a) Schematic diagram of experimental data collection, (b) Placement of electrodes for EMG signal acquisition, (c) EMG sensors, (d) IMU, (e) Time and sequence of actions performed by the user in a single trial.

2) Feature extraction

Following filtering, the sEMG signals were processed using overlapping analysis windows with a window length of 200 milliseconds and an increment of 40 milliseconds. To accurately estimate joint movement angles, it is necessary to extract a range of features from each data window in order to build a comprehensive feature vector. The time domain features, frequency domain, and time-frequency domain features have been extensively employed in processing sEMG signals [28, 29].

Time domain features are strongly correlated with the amplitude properties of sEMG signals and accurately convey angular information. Therefore, 14 time domain features were extracted from the surface EMG signal.These include MAV, RMS, ZC, SSC, WL, integrated EMG, variance, kurtosis, skewness, and five coefficients derived from autoregressive models. The extraction process for these features plays a crucial role in capturing vital information contained within sEMG signals that subsequently aids in estimating joint movement angles.

C. Modeling of the angle estimates based on sEMG

The Back Propagation Neural Network (BPNN), a widely utilized approach in supervised learning, is inspired by the simulation of activation and information transmission processes observed in human neurons. As a shallow feedforward neural network, BPNN adjusts its weights through the backpropagation algorithm to learn and adapt to complex patterns present in input data, thereby playing a pivotal role in machine learning and pattern recognition. The structure comprises an input layer for receiving data, a hidden layer bridging input and output layers with multiple neurons, and an output layer for generating final predictions. In this study, employed the

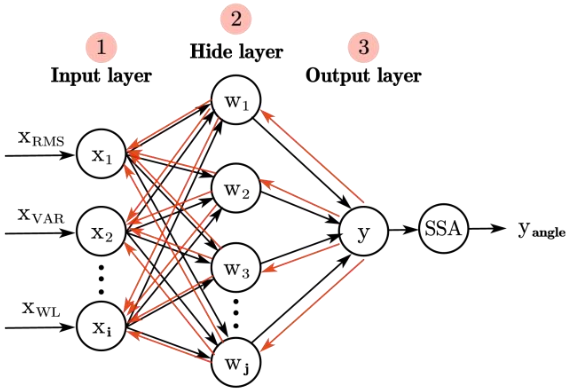

Figure 3. Schematic diagram of the BPNN _ SSA algorithm.

classical architecture of a BPNN. Through BPNN, estimated angles of the four finger joints can be calculated. However, it is important that angle curves generated by BPNN exhibit fluctuations; thus, a smoothing method is required to process the predicted angle signals. SSA stands as a non-parametric approach that breaks down the original time series into constituent parts, allowing for the differentiation between informative components and noise within the signals. Additionally, SSA facilitates signal smoothing [30], capturing the trend of the signal. Therefore, the SSA method is used in this study to optimize the fluctuations generated by BPNN. As illustrated in Figure 3, this represents the angle prediction framework based on the BPNN_SSA model.

SSA is a non-parametric method used for analyzing time series data. It combines techniques from classical time series analysis and multivariate statistical analysis, primarily employed to identify and extract trends, periodic components, and noise in time series. The basic principles of SSA are as follows:

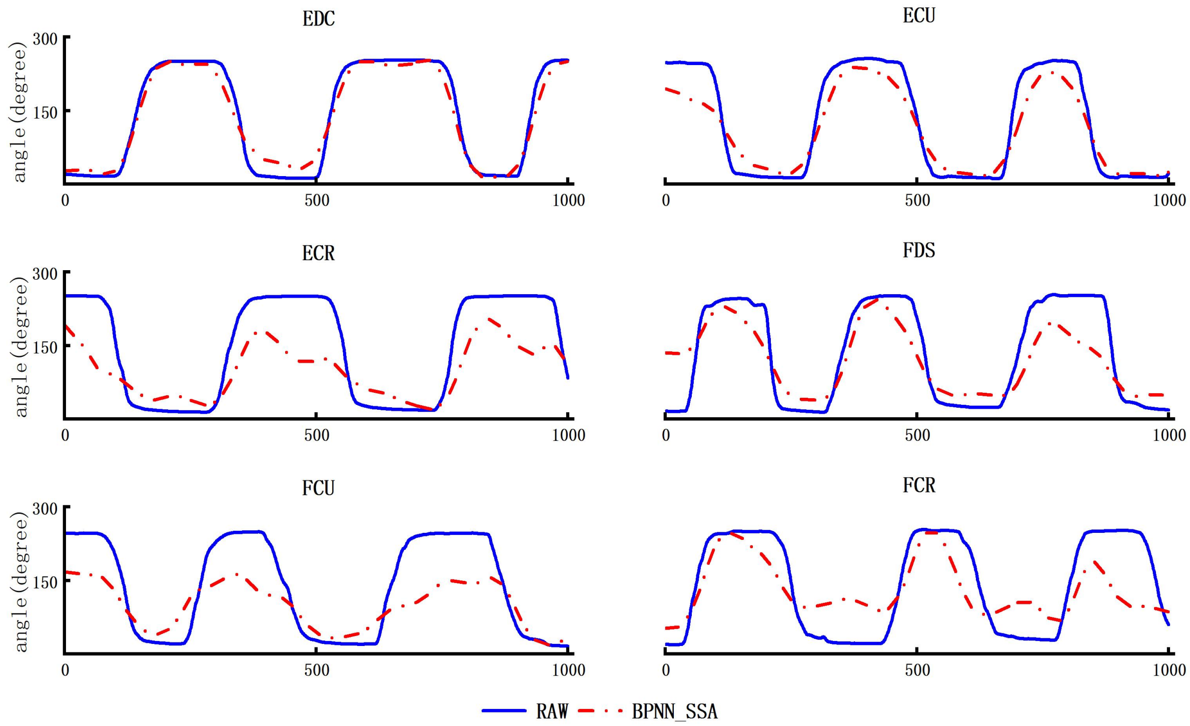

Figure 4. Comparative Analysis of Four-Finger Joint Angle Estimates from Six Single-Channel BPNN_SSA Models

Firstly, one chose an appropriate length L as the sliding window (with a step size of 1) and cut the original time series of length N into K consecutive sub-sequences. These sub-sequences were then arranged to form an L-row and K-column trajectory matrix *X*. Where K=N-L+1.

$$X=[X_1\cdots X_K]=(x_{ij})_{i,j=1}^{L,K}=\begin{pmatrix} x_1 & x_2 & x_3 & \cdots & x_K \\ x_2 & x_3 & x_4 & \cdots & x_{K+1} \\ x_3 & x_4 & x_5 & \cdots & x_{K+2} \\ \vdots & \vdots & \vdots & \ddots & \vdots \\ x_L & x_{L+1} & x_{L+2} & \cdots & x_N \end{pmatrix} \tag{1}$$

Next, $S = XX^T$ was calculated, and then eigenvalue decomposition was performed on matrix S to obtain a set of eigenvalues $\lambda_1 > \lambda_2 > \cdots > \lambda_L \gg 0$ sorted in descending order, along with their corresponding eigenvectors $U_1, U_2, U_3, \ldots, U_L$.Using these eigenvalues and eigenvectors, the trajectory matrix X can be decomposed via singular value decomposition to obtain

$$X = X_1 + X_2 + \cdots + X_d \tag{2}$$

Where $d = \min\{L, k\}$, $X_i = \sqrt{\lambda} U_i V_i^T$, U_i is the left singular vector of X_i, V_i is the right singular vector of X_i, and $\sqrt{\lambda}$ is the singular value corresponding to X_i.

Subsequently, in the singular spectrum, higher singular values generally indicate significant components with large amplitudes in the decomposition. In contrast, lower singular values are associated with noise components of small amplitudes in the signal. Consequently, for signal smoothing, one can reconstruct the signal by considering the size of the singular values and disregarding the sub-sequences with lower singular values deemed as noise, thereby attaining the objective of smoothing the signal. Hence, the modified trajectory matrix is

$$X' = X_1 + X_2 + X_3 + \cdots + X_r \tag{3}$$

Where r<d. Subsequently, the diagonal averaging operation is performed on the processed trajectory matrix to convert the matrix data to the original time series form of length N.

$$y_k = \begin{cases} \dfrac{1}{k}\sum_{m=1}^{k} X'_{m,k-m+1}, & 1 \le k < L \\ \dfrac{1}{L}\sum_{m=1}^{L} X'_{m,k-m+1}, & L \le k \le K \\ \dfrac{1}{N-k+1}\sum_{m=k-K+L}^{N-K+1} X'_{m,k-m+1}, & K < k \le N \end{cases} \tag{4}$$

The goal of smoothing the forecast data can be achieved through the above steps.

D. Evaluation criteria

The training model and additional test performance were evaluated using the Normalized Root Mean Square Error (NRMSE) and the Coefficient of Determination (R^2), each providing an independent assessment of the model's estimation capabilities post-training. NRMSE reflects the deviation in joint angles between the measured and estimated four-finger joints, expressed as a percentage (%). R^2 assesses the model's fit to the data; when R^2 approaches 1, it indicates that it fits the data well, meaning the predicted values closely align with the observed values.

$$R^2 = 1 - \frac{\sum_{i=1}^{N}(x_i - y_i)^2}{\sum_{i=1}^{N}(x_i - \bar{x})^2} \tag{5}$$

$$NRMSE = \frac{\sqrt{\frac{1}{N}\sum_{i=1}^{N}(y_i - x_i)^2}}{x_{\max} - x_{\min}} \tag{6}$$

Here, x_i represents the observed value of the actual finger joint angle for the i-th data point, $\bar{x}$ denotes the arithmetic mean of the actual finger joint angles across all data points; y_i i represents the predicted finger joint angle value from the model for the i-th data point, $\bar{y}$ denotes the arithmetic mean of the predicted values from the model across all data points, and N represents the total number of data points in the dataset.

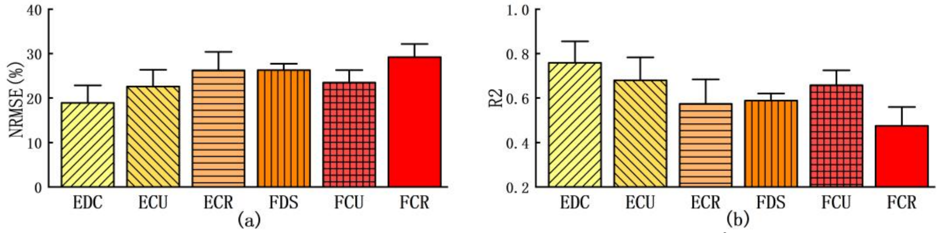

Figure 5. Compares the estimation accuracy of sEMG signals across six channels. (a) NRMSE values, (b) R^2 values. Bar graphs represent means, and error bars are the standard error of the mean.

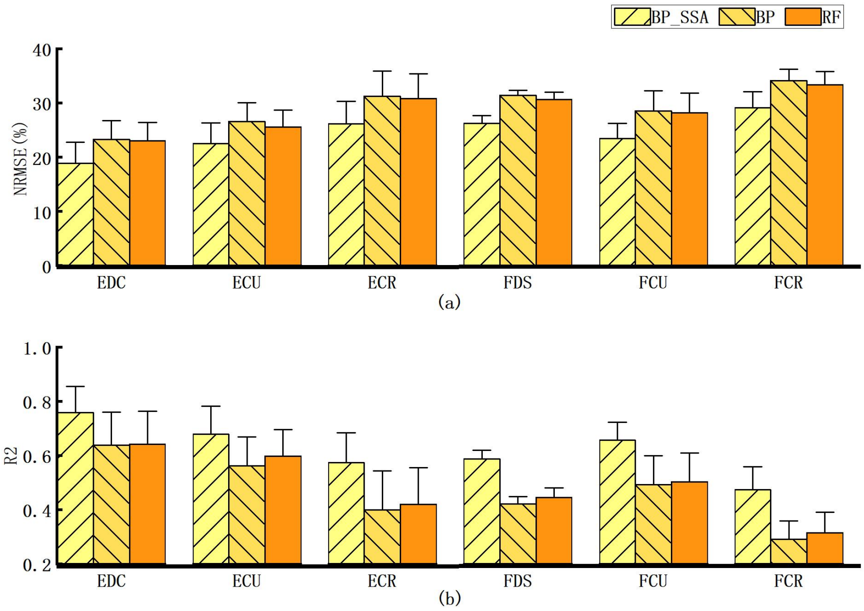

Figure 6. Comparison of angle estimation accuracy across six channels for three models. (a) NRMSE values, (b) R^2 values. Bar graphs represent the means, and error bars indicate the standard error of the mean.

III. Experiments and Results

A. Experimental processing

This study employed Random Forest (RF) and BPNN regression models. For the RF predictions, we set the number of decision trees to 100 and established 5 leaf nodes. In the BPNN prediction phase, the model was configured with 30 hidden layers, 1000 iterations were performed, and an error threshold of 0.000001 was set, along with a learning rate of 0.01. In terms of data collection, over 12000 samples were gathered for each channel, which is approximately equivalent to 10 minutes of data. For model training, preprocessed data from each channel was used as a separate input. Additionally, the dataset was divided into five groups using a 5-fold cross-validation method for predictive analysis.

B. Comparison of Prediction Results Across Different Channels

Figure 4 provides an intuitive comparison of the four-finger joint angle data from six arm regions of Subject 1, derived from direct measurements using IMUs and predictions generated by the BPNN_SSA model. This comparison highlights discrepancies between the predicted and actual joint angles across various channels, exhibiting varying degrees of deviation. Notably, the EDC muscle area predictions closely align with IMU measurements, while predictions for other areas show greater divergence from actual angles. To rigorously assess and compare these prediction differences across different channels, this study employed NRMSE and R^2 as evaluation metrics, with results presented in Figure 5. This figure comprehensively illustrates NRMSE and R^2 values for each channel location when using the BPNN_SSA model for predictions.

In summary, although all channel locations demonstrated a certain level of predictive accuracy, the EDC area exhibited particularly strong performance. Specifically, the average NRMSE for the EDC region was recorded at only 18.9%, which is significantly lower than that observed in other channel locations—indicating superior prediction accuracy. Concurrently, the average R^2 for the EDC area reached 0.756, close to 1 and markedly surpassing those of other channels; this further corroborates its enhanced angle estimation capability at this site. These quantitative evaluation results clearly underscore the exceptional performance of angle estimation within the EDC location relative to other areas.

C. Comparison of Results from Different Models

This experiment investigated the potential of the SSA algorithm to enhance the performance of the BPNN model, establishing both the BPNN model and Random Forest as comparative benchmarks. Figure 6 clearly illustrates the NRMSE and R^2 metrics for three models in predicting finger angle across six arm regions. The results indicate that prior to applying SSA smoothing, both the BPNN model and RF exhibited comparable prediction performance with no significant differences observed. However, when integrating the SSA algorithm with the BPNN model to create the BPNN_SSA model, there was a marked improvement in prediction performance across all

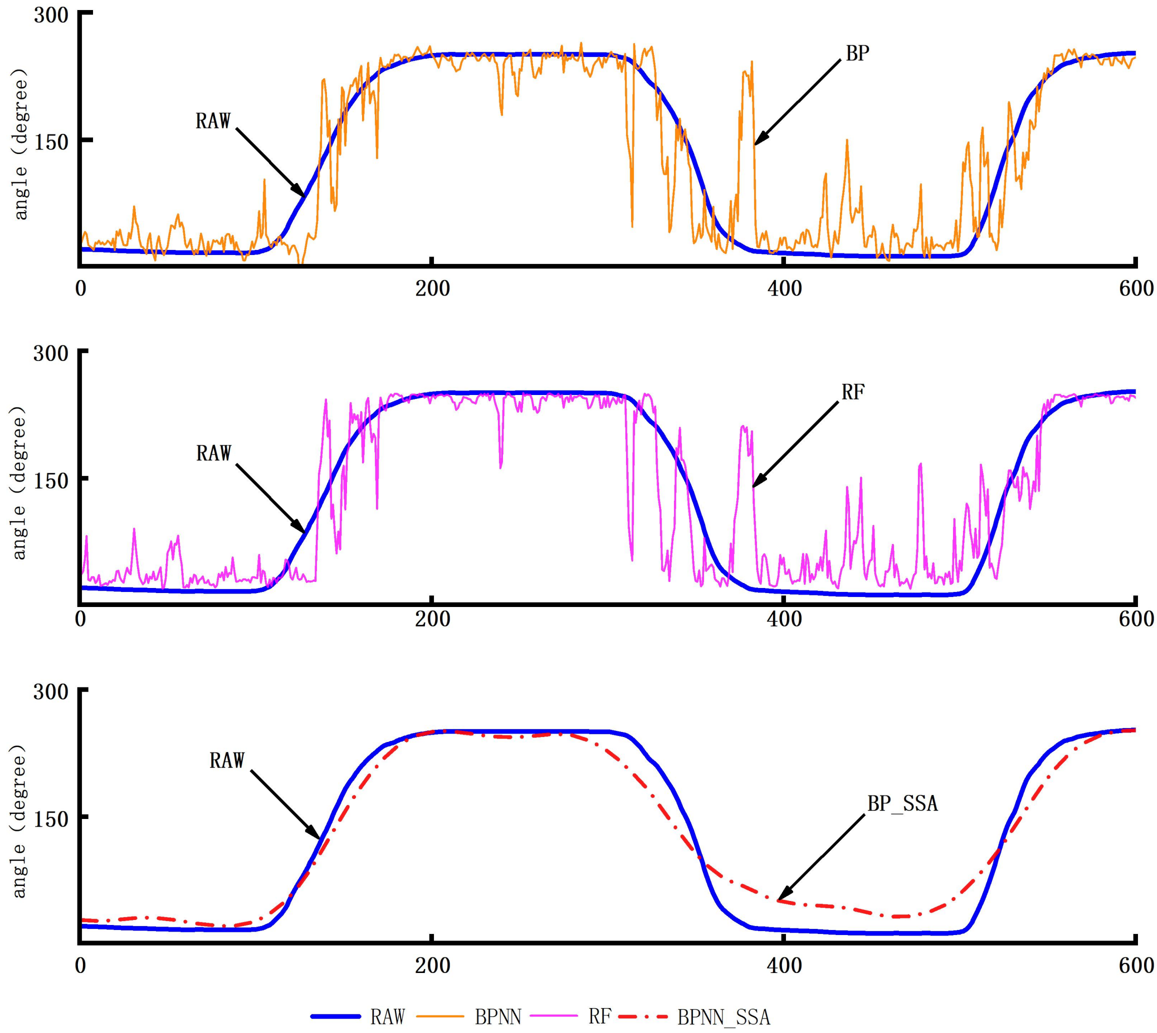

Figure 7. Comparison of Four-Finger Joint Angles at the Finger Extensor Area Between Different Models.

six arm regions. Furthermore, Figure 7 compares prediction results for these three models at the EDC site. Before implementing SSA smoothing, both the BPNN and RF models displayed considerable fluctuations and deviations in their predictions; conversely, the BPNN_SSA model demonstrated a substantial ability to smooth out these predictions and reduce errors significantly. These findings strongly affirm the SSA algorithm's effectiveness in enhancing the BPNN model's predictive capabilities.

IV. Discussion

A. Feasibility of Single-Channel Semg Estimation

In practical applications, the effectiveness of sEMG signals is often limited by factors such as muscle activity status, mechanical noise, and system architecture complexity. These limitations pose significant challenges to their application. Therefore, it is necessary to consider methods that utilize a small number of channels or even single-channel sEMG signals. However, compared to multi-channel signals, the amount of feature information that can be extracted from a single channel is considerably reduced, raising concerns about its ability to reflect continuous changes in finger joint angles accurately. This study selected simple four-finger movements as a research case to address this issue, as depicted in Figure 2. The experimental findings indicate that the method proposed in the present study is capable of accurately forecasting finger joint angles for these simple motion patterns(as shown in Figure 7). This finding indicates the feasibility of using single-channel sEMG signals to predict finger movements.

B. Effectiveness of Signal Smoothing Processing

During continuous finger motion estimation, details of muscle activity captured through feature extraction employing single-channel sEMG are relatively limited. This limitation often leads to fluctuations in the prediction output of the training model. As illustrated in Figure 7, signals that lack smoothing processing can result in significant fluctuations and even deviations in prediction results, thereby considerably reducing the accuracy of angle estimation. However, incorporating signal smoothing techniques can substantially improve this situation and reduce error margins. Smoothing processing serves as a filtering method designed to retain the core characteristics of a signal while emphasizing its overall trend. Digital Butterworth filters, spline interpolation methods, and spectrum-based filters are common smoothing techniques in this context. Notably, when addressing non-stationary signals such as sEMG, spline interpolation methods frequently demonstrate superior smoothing effects. Therefore, spline smoothing based on the SSA method can effectively capture the signal trend when processing sEMG signals. Especially when the predicted result is close to the actual observation result, the smoothing effect provided by SSA is particularly obvious. For instance, when utilizing sEMG signals from the EDC channel to predict joint angles, the resulting angle curve exhibits high consistency with data curves obtained through an IMU, as depicted in Figure 7. Therefore, by implementing signal smoothing processes, both accuracy and stability in four-finger joint angle estimation can be significantly enhanced—bringing prediction outcomes closer to real-world measurements.

C. Issues in Finger Angle Estimation

Although this experiment has made significant progress in exploring single-channel motion estimation, several key challenges remain to be addressed. The primary challenge pertains to the relatively simplistic finger movement patterns utilized in the experiment, which do not adequately encompass the complex and variable movements of finger joints encountered in real-world scenarios. Additionally, experimental data collection was confined to a single session, failing to sufficiently account for potential shifts in data distribution caused by factors such as fatigue, environmental changes, or variations in collection position over time; these factors can adversely affect the accuracy of prediction results. Furthermore, while models trained separately for each participant exhibited commendable predictive performance, substantial inter-individual differences in data may result in diminished model efficacy when applied to predictions across different subjects. Therefore, future research will concentrate on developing a more universal and accurate model to enhance the precision of finger joint angle estimation using single-channel sEMG signals and ensure that this model can be broadly and effectively adapted for diverse subjects.

V. CONCLUSION

In this paper, a prediction algorithm for four-finger joint motion estimation using single channel sEMG signal combined with BPNN and SSA is proposed. To evaluate the performance of this approach, sEMG signals were recorded from six distinct muscles: EDC, ECR, ECU, FDS, FCR, and FCU. The proposed BPNN_SSA algorithm was then employed to estimate four-finger joint movements. Experimental results demonstrate that the BPNN algorithm incorporating the SSA smoothing method outperforms both traditional BPNN and RF algorithms in estimating four-finger movements. Furthermore, the proposed BPNN_SSA method effectively estimates four-finger motion using sEMG signals from the EDC muscle, with a mean NRMSE of 18.9% and a mean R^2 value of 0.758. In summary, the BPNN_SSA algorithm based on single channel sEMG signal can predict the continuous motion of four fingers.

REFERENCES

[1] Thomas B Sheridan, "Human-Robot Interaction: Status and Challenges," Human factors, vol. 58, no.4, pp525-532, 2016

[2] Jihong Zhu, Ben jamin Navarro, Robin Passama, Philippe Fraisse, Crosnier Andre, Cherubini Andrea, "Robotic Manipulation Planning for Shaping Deformable Linear Objects WithEnvironmental Contacts," IEEE Robotics and Automation Letters, vol. 5, no.1, pp16-23, 2020

[3] Nan Gu, Zhouhua Peng, Dan Wang, et al., "Path-Guided Containment Maneuvering of Mobile Robots: Theory and Experiment," IEEE Transactions on Industrial Electronics, vol. 68, no.8, pp7178-7187, 2021

[4] Subasi Abdulhamit, "Diagnosis of Neuromuscular Disorders Using DT-CWT and Rotation Forest Ensemble Classifier," IEEE Transactions on Instrumentation and Measurement, vol. 69, no.5, pp1940-1947, 2020

[5] Pasinetti Simone, Matteo Lancini, Ileana Bodini, Franco Docchio, "A Novel Algorithm for EMG Signal Processing and Muscle Timing Measurement," IEEE Transactions on Instrumentation and Measurement, vol. 64, no.11, pp2995-3004, 2015

[6] Jeff Kilby, Krishnamachar Prasad, Grant Mawston, "Multi-Channel Surface Electromyography Electrodes: A Review," IEEE Sensors Journal, vol. 16, no.14, pp5510-5519, 2016

[7] Jaemin Lee, Minkyu Kim, et al., "A Control Scheme to Minimize Muscle Energy for Power Assistant Robotic Systems Under Unknown External Perturbation," IEEE Transactions on Neural Systems and Rehabilitation Engineering, vol. 25, no.12, pp2313-2327, 2017

[8] Lobo-Prat Joan, Nizamis Kostas, et al., "Comparison between sEMG and force as control interfaces to support planar arm movements in adults with Duchenne: a feasibility study," Journal of NeuroEngineering and Rehabilitation, vol. 14, no.1, pp73, 2017

[9] V. R. Jayaneththi, J. Viloria, L. G. Wiedemann, C. Jarrett, A. J. McDaid, "Robotic assessment of neuromuscular characteristics using musculoskeletal models: A pilot study," Computers in Biology and Medicine, vol. 86, pp82-89, 2017

[10] Khoshdel Vahab, Akbarzadeh Alireza, Naghavi Nadia, et al., "sEMG-based impedance control for lower-limb rehabilitation robot," Intelligent Service Robotics, vol. 11, no.1, pp97-108, 2018

[11] Dezhen Xiong, Daohui Zhang, Xingang Zhao, et al., "Deep Learning for EMG-based Human-Machine Interaction: A Review," IEEE/CAA Journal of Automatica Sinica, vol. 8, no.3, pp512-533, 2021

[12] Yingwei Zhang, Yiqiang Chen, Hanchao Yu, Xiaodong Yang, Lu Wang, "Learning Effective Spatial-Temporal Features for sEMG Armband-Based Gesture Recognition," IEEE Internet of Things Journal, vol.7, no.8, pp6979-6992, 2020

[13] Luzheng Bi, Aberham Genetu Feleke, Cuntai Guan, "A review on EMG-based motor intention prediction of continuous human upper limb motion for human-robot collaboration," Biomedical Signal Processing and Control, vol. 51, pp113-127, 2019

[14] Xugang Xi, Chen Yang, Seyed M. Miran, Yun-Bo Zhao, Shuliang Lin, et al., "sEMG-MMG State-Space Model for the Continuous Estimation of Multijoint Angle, "Complexity," vol. 2020, no.2020, pp1-12, 2022

[15] David Hofmann, Ning Jiang, Ivan Vujaklija, Dario Farina, "Bayesian Filtering of Surface EMG for Accurate Simultaneous and Proportional Prosthetic Control," IEEE Transactions on Neural Systems and Rehabilitation Engineering, vol. 24, no.12, pp1333-1341, 2016

[16] Yongsheng Gao, Yang Luo, Jie Zhao, Qiang Li, "sEMG-angle estimation using feature engineering techniques for least square support vector machine," Technology and Health Care, vol. 27, no.s1, pp31-46, 2019

[17] Zixuan Qin, Sorawit Stapornchaisit, Zixun He, et al., "Multi-Joint Angles Estimation of Forearm Motion Using a Regression Model," Frontiers in Neurorobotics, vol. 15, pp685961, 2021

[18] Qin Zhang, Li Fang, Qining Zhang, Caihua Xiong, "Simultaneous estimation of joint angle and interaction force towards sEMG-driven human-robot interaction during constrained tasks," Neurocomputing, vol. 484, pp38-45, 2022

[19] Pengjie Qin, Xin Shi, "A Novel Method for Lower Limb Joint Angle Estimation Based on sEMG Signal," IEEE Transactions on Instrumentation and Measurement, vol. 70, pp1-7, 2021

[20] Hai Wang, Qing Tao, Na Su, Xiaodong Zhang, "Simultaneous Estimation of Hand Joints Angles Toward sEMG-Driven Human-Robot Interaction," IEEE Access, vol. 10, pp109385-109394, 2022.

[21] Fei Wang, Tenglong Yin, Chenxi Lei, Yuanke Zhang, Yifan Wang, Jian Liu, "Prediction of lower limb joint angle using sEMG based on GA-GRNN," Lecture Notes in 2015 IEEE International Conference on Cyber Technology in Automation, Control, and Intelligent Systems (CYBER), 08-12 June, 2015, Shenyang, China, pp1894-1899

[22] Feiyun Xiao, Yong Wang, Yongsheng Gao, Yanhe Zhu, Jie Zhao, "Continuous Estimation of Elbow Joint Angle by Multiple Features of Surface Electromyographic Using Grey Features Weighted Support Vector Machine," Journal of Medical Imaging and Health Informatics, vol. 7, no.3, pp574-583, 2017

[23] Dario Farina, Ning Jiang, Hubertus Rehbaum, Ales Holobar, et al., "The Extraction of Neural Information from the Surface EMG for the Control of Upper-Limb Prostheses: Emerging Avenues and

Challenges," IEEE Transactions on Neural Systems and Rehabilitation Engineering, vol. 22, no.4, pp797-809, 2014
[24] Song Zhang, Ningbo Yu, Zhenhui Guo, Weiguang Huo, Jianda Han, "Single-Channel sEMG-Based Estimation of Knee Joint Angle Using a Decomposition Algorithm With a State-Space Model," IEEE Transactions on Neural Systems and Rehabilitation Engineering, vol. 31, pp4703-4712, 2023
[25] Song Zhang, Jiewei Lu, Weiguang Huo, Ningbo Yu, Jianda Han, "Estimation of knee joint movement using single-channel sEMG signals with a feature-guided convolutional neural network," Frontiers in Neurorobotics, vol. 16, 2022
[26] Junkai Shao, Yafeng Niu, Chengqi Xue, Qun Wu, Xiaozhou Zhou, Yi Xie, Xiaoli Zhao, "Single-channel SEMG using wavelet deep belief networks for upper limb motion recognition," International Journal of Industrial Ergonomics, vol. 76, pp102905, 2020
[27] Yansheng Wu, Shili Liang, Ling Zhang, Zongqian Chai, Chunlei Cao, Shuangwei Wang, "Gesture recognition method based on a single-channel sEMG envelope signal," EURASIP Journal on Wireless Communications and Networking, vol. 2018, no.1, pp35, 2018
[28] Angkoon Phinyomark, Rami N Khushaba, Erik Scheme, "Feature Extraction and Selection for Myoelectric Control Based on Wearable EMG Sensors," Sensors, vol. 18, no.5, pp1615, 2018
[29] Jongman Kim, Bummo Koo, Yejin Nam, Youngho Kim, "sEMG-Based Hand Posture Recognition Considering Electrode Shift, Feature Vectors, and Posture Groups," Sensors, vol. 21, no.22, pp7681, 2021
[30] F. Romero, F. J. Alonso, et al., "An automatic SSA-based de-noising and smoothing technique for surface electromyography signals," Biomedical Signal Processing and Control, vol. 18, pp317-324, 2015

Lei Zhang worked in Xi’an Polytechnic University. He received Ph.D. and Maste’sr degree in Mechatronic Engineering from Northwestern Polytechnical University in 2020 and 2015. His research interests mainly include using surface electromyography signals to control exoskeletons and assist stroke patients/astronauts in rehabilitation training. The author has no conflict of interest.